

Supporting Information for “Charge-Transfer Heptamethine Dyes for NIR Singlet Oxygen Generation”

John B. Jarman and Dennis Dougherty

Table of Contents

Experimental Details	S2
Supporting Figures	S5
Figure S1	S5
Figure S2	S6
Figure S3	S6
Figure S4	S7
Figure S5	S7
Figure S6	S8
Figure S7	S8
Figure S8	S9
Figure S9	S10
References	S11

Experimental Details

Materials and Methods

IR-1061 tetrafluoroborate and dry pyridine were purchased from Sigma Aldrich. Acridine was purchased from Alfa Aesar. Sodium BArF was purchased from AK Scientific. Deuterated solvents were purchased from Cambridge Isotopes. Deuterated chloroform was filtered through a neutral alumina plug prior to use to neutralize and dry the solvent. Irradiations at 980 nm were performed using a 1 watt/cm² infrared diode laser at 980 nm coupled to a PSU-III-FDA power supply. Both the laser and the power supply were purchased from CNI lasers. Irradiations at 1064 nm were performed using an Nd:YAG laser at 1.8 W/cm². Absorbance spectra were obtained using an Agilent CARY 60 UV-Vis for spectra below 1000nm, and a Cary 5000 UV-VIS-NIR for spectra above 1000 nm. Mass spectrometry characterization was performed via MALDI using a BRUKER MALDI/TOF Autoflex Speed and a Waters LCT Premier XE Electrospray TOF. ¹H NMR spectra were obtained using a Varian 600 MHz Spectrometer.

Calculations:

Computation was performed using the SPARTAN interface with calculations performed using the B3LYP functional and the 6-31G** basis set. These calculations were performed in accordance with previous calculations performed on the 9-mesityl-10-methylacridinium dyad.¹ Higher levels of computation (using the MO6 functional and larger basis sets) were performed on the BODIPY dyads to check for differences, and none were observed. Given the large size of the IR-1061 dye and the lack of significant differences in higher level calculations, we felt that B3LYP and 6-31G** were the most appropriate selection.

Irradiation Experiments:

Dye was dissolved in deuterated solvent at a concentration that would produce an absorbance near 1 at 980 nm. This was calculated using extinction coefficients determined by absorbance measurements of the dye alone. The IR-1061-acridinium irradiation in water was an exception, as the concentration was kept lower to ensure solubility. Dye solution was split into two aliquots and added to two 1 cm by 1 cm quartz cuvettes purchased from Starna. The absorption spectra were taken for both cuvettes (to ensure the pre-irradiation sample looked the same in both cases), and subsequently one cuvette was irradiated while the other was kept in the dark. A stir bar was used to ensure proper mixing during irradiation. After irradiation, the absorbance of both solutions was again evaluated. Figures shown without a dark control still had one, however, no significant change was observed in the irradiated sample so the dark control trace was unnecessary and therefore not included. For the 1064 nm irradiation, the dye was dissolved at a slightly higher concentration to an absorbance of approximately 1.5 at 1064 nm and irradiated for 5 minutes. At this point significant photobleaching of the dye was observed, so additional irradiation was not performed.

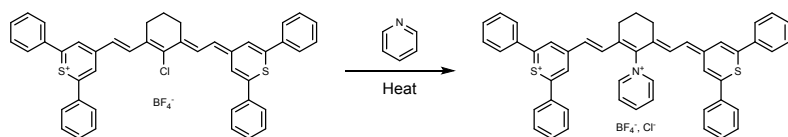
The freeze-pump-thaw (FPT) experiment was carried out as follows. Dye was dissolved in deuterated chloroform and added to a FPT that apparatus. Three consecutive freeze-pump-thaw cycles were carried out to a pressure of less than 200 mm Hg, at which point the solution was transferred under vacuum to the arm of the apparatus containing a fused 1 cm by 1 cm quartz cuvette (Starna). Irradiation and subsequent absorption measurements were carried out in the sealed cuvette.

Comparative Quantum Yield Experiments:

Phenalenone (Sigma-Aldrich), a highly efficient singlet oxygen generator with a known singlet oxygen quantum yield of .97 in chloroform² was used to benchmark the efficiency of IR-1061-acridinium singlet oxygen generation in chloroform. A solution of phenalenone at an absorbance of 0.30 at 365 nm was generated that also contained DPBF at an absorbance of approximately 1.0. This solution was irradiated for 30 seconds using a 365 nm variable power LED (3-300 mW, Thor labs) at 30 mW/cm². The percent decrease in DPBF signal at 415 nm was calculated, taking into account any background from phenalenone. This was done in triplicate. A similar experiment was then run using IR-1061-acridinium. A solution containing the dye at an absorbance of 0.30 at 1064 and DPBF at an absorbance of approximately 1.0 was irradiated for 30 seconds using a 1064 nm Nd:YAG laser with a power output of 1.8 W/cm². The percent decrease in DPBF signal at 415 nm was then calculated, taking into account any background from IR-1061-acridinium. This was also done in triplicate.

The percent decrease attributed to phenalenone was calculated to be 0.53 and the percent decrease attributed to IR-1061-acridinium was calculated to be 0.29 (Figure S8). To take into account the difference in photon flux at these two wavelengths, the ratio of the photon flux was calculated, where the photon flux was described by the following equation: $PF = I \cdot \lambda / (h \cdot c \cdot N_a)$. PF stands for photon flux, I is the irradiation intensity, λ is the irradiation wavelength, h is Planck's constant, c is the speed of light and N_a is Avogadro's number. The ratio of the photon flux was simplified to $PF_R = (I_{Phe} \cdot \lambda_{Phe}) / (I_{IR} \cdot \lambda_{IR}) = (0.03 \text{ W/cm}^2 \cdot 365 \text{ nm}) / (1.8 \text{ W/cm}^2 \cdot 1064 \text{ nm}) = 0.006$. Taking into account this difference in photon flux and phenalenone's known quantum yield of singlet oxygen generation of 0.97, this yields a relative quantum yield of about 0.003, or 0.3%.

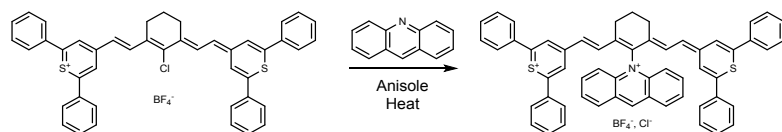
IR-1061-pyridinium synthesis:



A 10 mL flame-dried round-bottom flask was charged with a stir bar and 25 mgs of IR-1061, to which 1 milliliter of dry pyridine was added. The reaction was heated to boiling under argon, and removed from heat once the solution transitioned from dark red to greenish-brown. At this point the compound was purified by silica gel chromatography using a 0-5% MeOH in DCM gradient. The product could not be cleanly purified due to decomposition during purification. All other attempted purification conditions gave the same result. Due to low solubility and contaminating species, an interpretable NMR was never obtained, however, a reasonably clean mass spectrometry trace was.

MS (MALDI-TOF): (m/z) calculated for C₄₉H₃₈NS₂⁺: 704.24 (m-1). Observed 704.056 (m-1, presumably due to loss of a proton to alleviate the dual positive charge) (Figure S4).

IR-1061-acridinium synthesis:

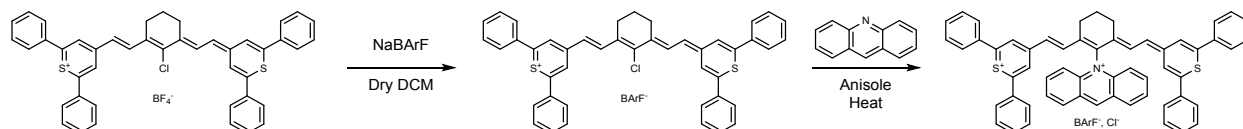


A 10 ml round-bottom flask was charged with a stir bar, 25 mgs of IR-1061 (1 equivalent), and 60 mgs of acridine (10 equivalents). Two milliliters of anisole were added, and the reaction was heated to boiling under argon. It was removed from heat once the color change from red to a yellow hued brown. Further heating led to formation of a green decomposition product. The reaction mixture was loaded onto a silica plug, and after eluting the anisole and any nonpolar compounds with DCM, a polar fraction containing the dye of interest was eluted with 5% MeOH in DCM. After pumping down, this polar fraction was resuspended in DCM and loaded onto a silica gel column, which was eluted with a 0-2% MeOH in DCM gradient. 20 mgs of pure product were collected as a brown-yellow compound, giving a percent yield of 64%.

¹H-NMR: 7.75 (m, 2H), 7.68-7.60 (m, 12H), 7.52-7.42 (m, 14 H), 6.99 (t, 2H) 6.91 (d, 2H), 6.65 (t, 2H), 6.59 (d, 2H), 6.28 (m, 1H), 2.84 (t, 2H), 2.56 (t, 2H), 1.95 (m, 2H)

MS (ESI-TOF): (m/z) calculated for C₅₇H₄₂NS₂⁺: 804.275 (m-1). Observed 804.277 (m-1, due to loss of a proton to alleviate the dual positive charge) (Figure S5).

IR-1061-acridinium BArF synthesis:



IR-1061 BArF was synthesized and purified in the manner described by Shi et al.³ Following isolation, 25 mgs of IR-1061 BArF (1 equivalent) was added to a 10 ml round-bottom flask along with a stir bar and 29.3 mgs of acridine (10 equivalents). Two milliliters of anisole were added, and the reaction was heated under argon. It was removed from heat once the color change from red to a yellow hued brown. Further heating led to formation of a green decomposition product. The reaction mixture was taken up in DCM and extracted three times with water and once with brine. The DCM fraction was pumped to near dryness, then resuspended in DCM and loaded onto a silica gel column. The product was eluted with a 0-1% MeOH in DCM gradient. 12 mgs of pure product were collected as a brown-yellow compound, giving a percent yield of 43%. NMR and mass spec data matched that of IR-1061-acridinium tetrafluoroborate, although significant peak broadening was observed on the MALDI with the BArF counterion.

¹H-NMR: 7.75 (m, 2H), 7.68-7.60 (m, 12H), 7.52-7.42 (m, 14 H), 6.99 (t, 2H) 6.91 (d, 2H), 6.65 (t, 2H), 6.59 (d, 2H), 6.28 (m, 1H), 2.84 (t, 2H), 2.56 (t, 2H), 1.95 (m, 2H)

MS (MALDI): (m/z) calculated for C₅₇H₄₂NS₂⁺: 804.275 (m-1). Observed 804.5 (m-1, due to loss of a proton to alleviate the dual positive charge).

Supporting Figures

Figure S1

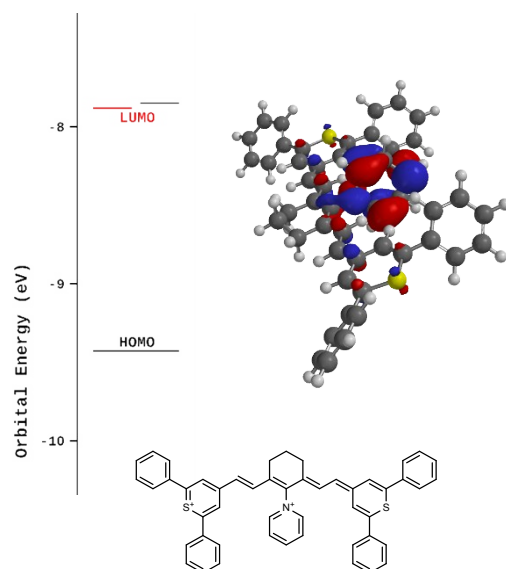
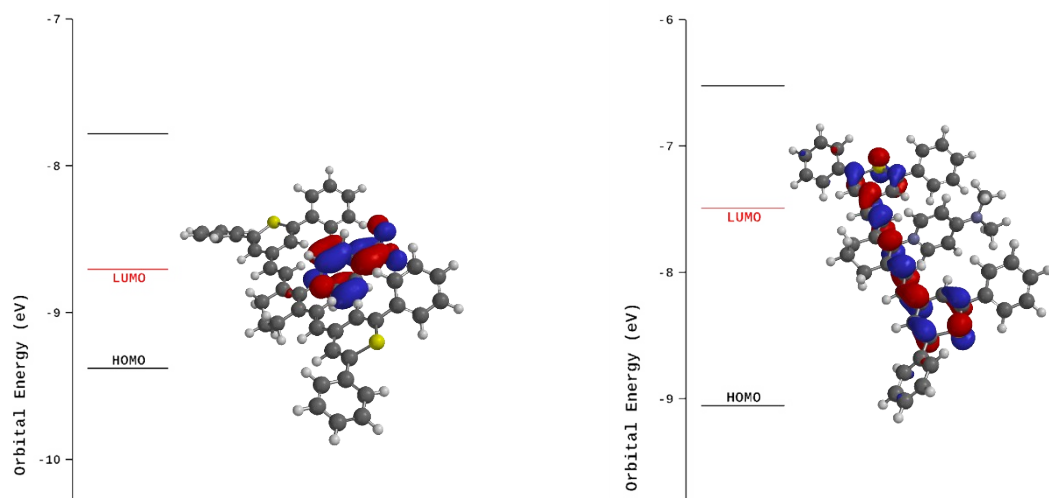
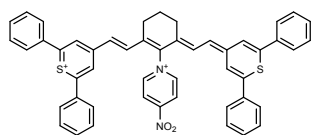


Fig S1. IR-1061-pyridinium orbital energies. Upon inverting the pyridine charge-transfer partner so that it is linked via an N-C bond instead of a C-C bond, similar orbitals are observed. As in IR-1061-CAT, the HOMO resides on the heptamethine backbone.

Figure S2



IR-1061-*p*-nitropyridinium



IR-1061-*p*-dimethylaminopyridinium

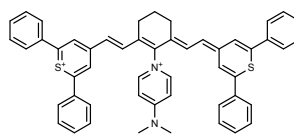


Fig S3. Representative IR-1061-pyridinium derivatives with electron withdrawing (*p*-nitro) and electron donating (*p*-dimethylamino) groups. Electron withdrawing groups reinforce frontier orbital orthogonality while electron donating groups do the opposite.

Figure S3

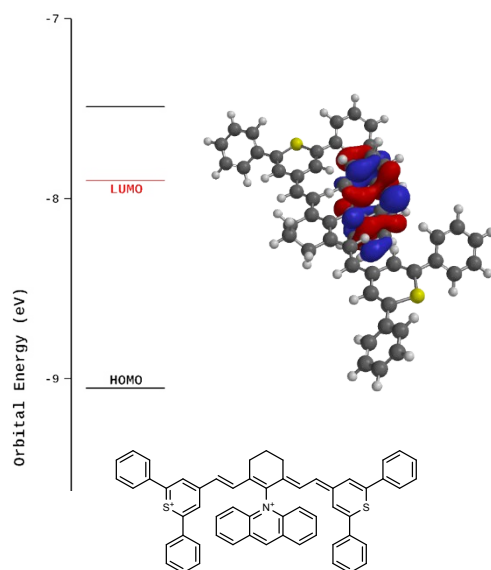


Fig S2. IR-1061-acridinium orbital energies. In IR-1061-acridinium the orthogonal orbital is heavily favored as the LUMO, suggesting the possibility of charge-transfer.

Figure S4

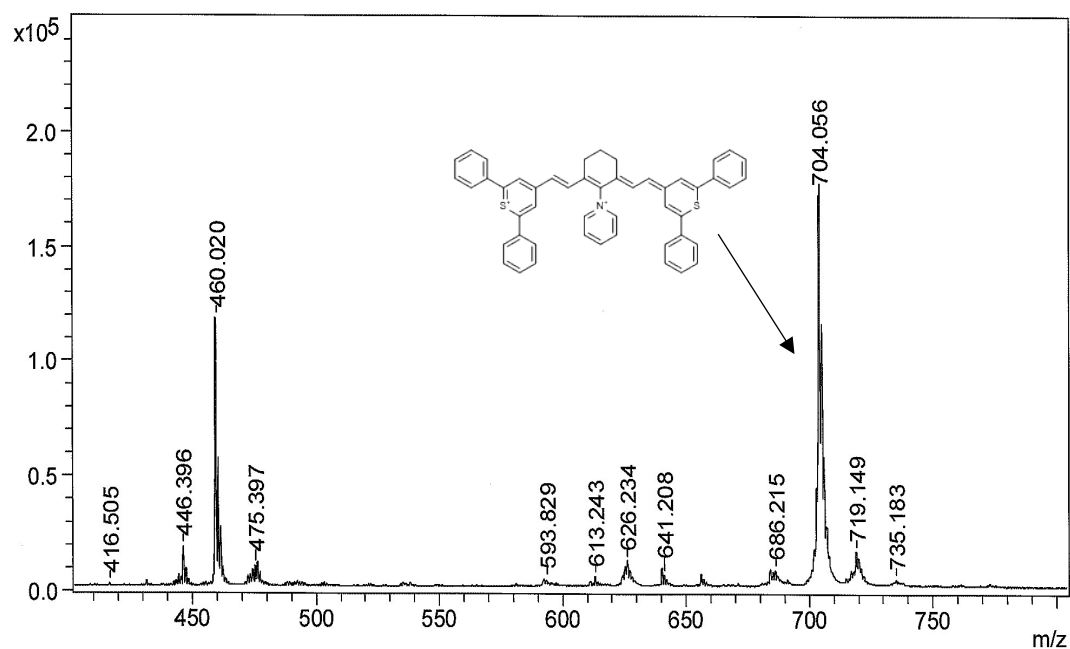


Fig S4. MALDI of slightly impure IR-1061 pyridinium. When isolated, the major impurity at 460 amu has no absorbance in the NIR.

Figure S5

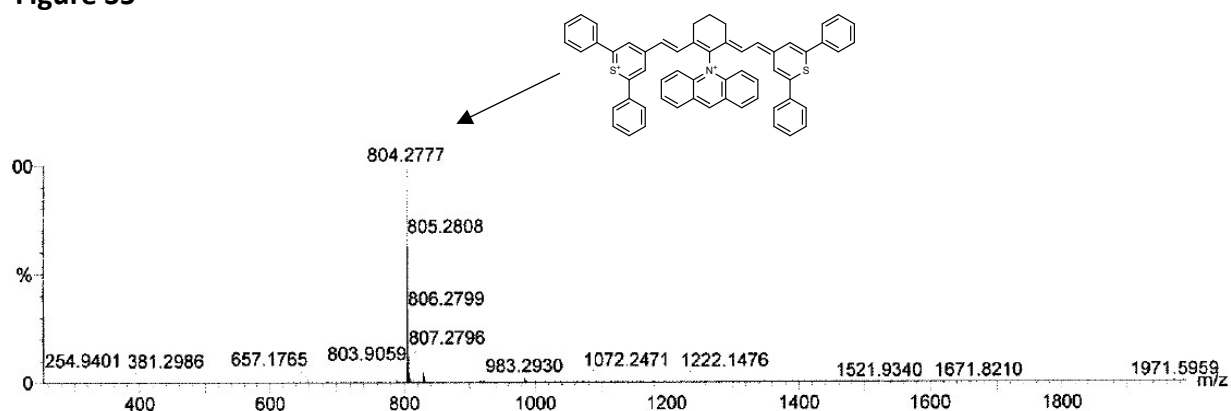


Fig S5. ESI/TOF of IR-1061-acridinium.

Figure S6

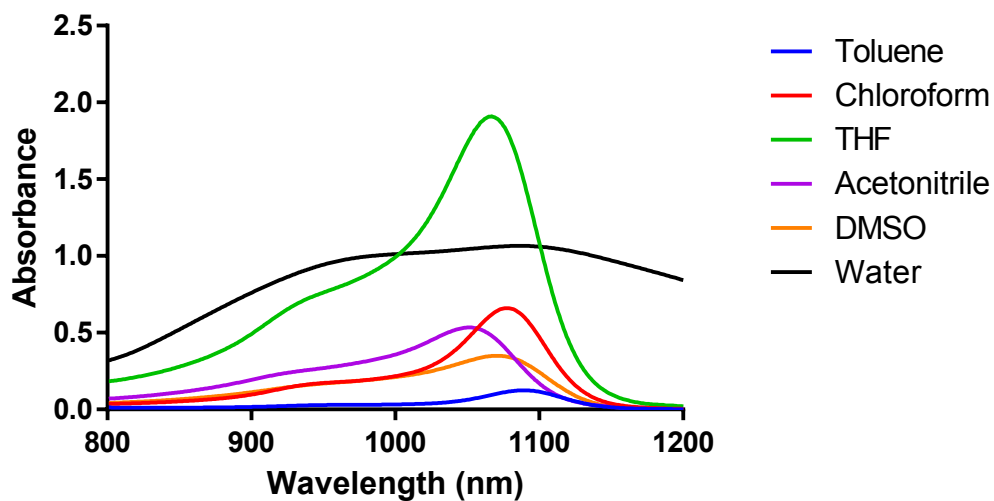


Fig S6. Absorption spectra of IR-1061-acridinium in different solvents at a concentration of .025 mg/ml. Most notable are the high extinction coefficient in THF and the extremely broad absorption spectrum in water.

Figure S7

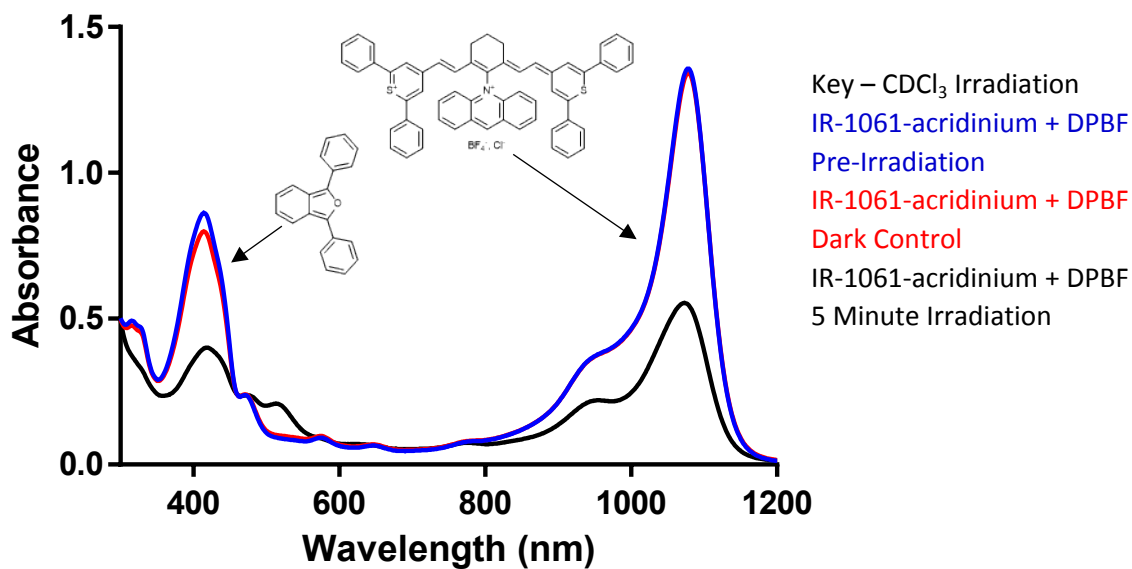


Fig S7. Irradiation of IR-1061-acridinium at 1064 nm in CDCl₃. Rapid bleaching of both the dye and DPBF signal was observed during irradiation.

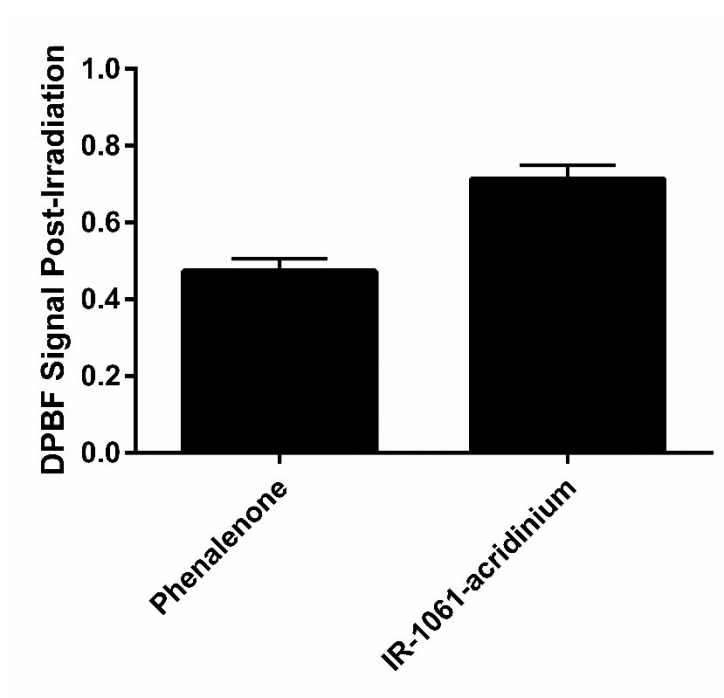


Figure S8

Fig S8. Normalized decrease in DPBF signal following irradiation in the presence of phenalenone and IR-1061-acridinium. An approximately 200-fold greater photon flux was used to irradiate IR-1061-acridinium.

Figure S9

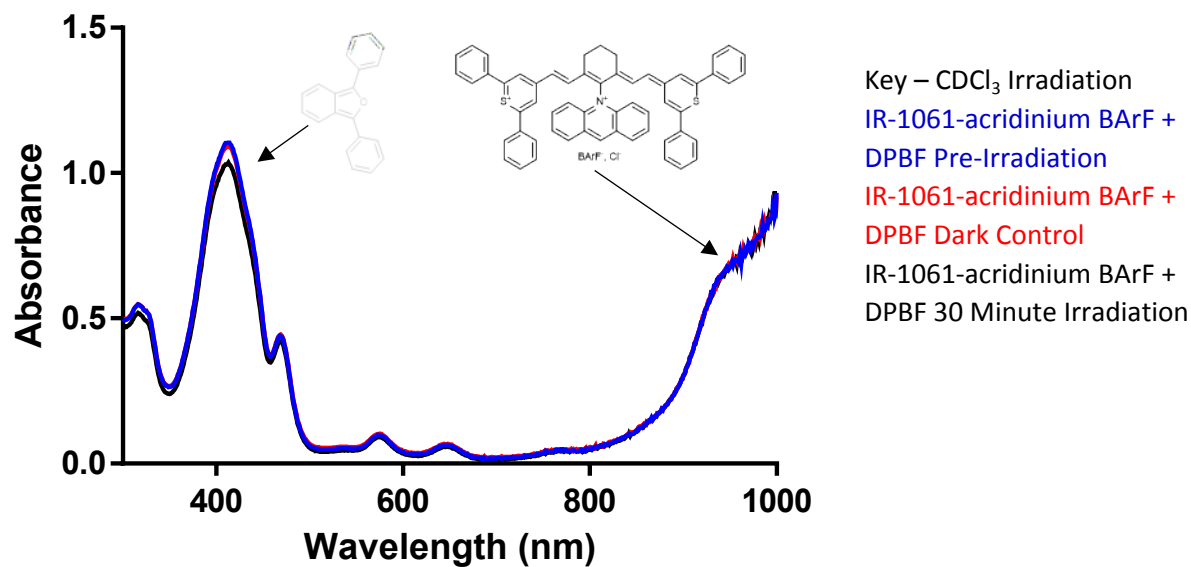


Fig S9. Irradiation of IR-1061-acridinium BArF at 980 nm in CDCl₃. Reactivity was significantly reduced upon exchanging the tetrafluoroborate counterion for a BArF counterion.

References

- 1 S. Fukuzumi, H. Kotani, K. Ohkubo, S. Ogo, N. V. Tkachenko and H. Lemmetyinen, *J. Am. Chem. Soc.*, 2004, **126**, 1600–1601.
- 2 R. Schmidt, C. Tanielian, R. Dunsbach and C. Wolff, *Journal of Photochemistry and Photobiology A: Chemistry*, 1994, **79**, 11–17.
- 3 Y. Shi, A. J.-T. Lou, G. S. He, A. Baev, M. T. Swihart, P. N. Prasad and T. J. Marks, *J. Am. Chem. Soc.*, 2015, **137**, 4622–4625.